blood

2009 114: 2542-2552
Prepublished online Jun 8, 2009;
doi:10.1182/blood-2009-03-213934

Successful treatment of the murine model of cystinosis using bone marrow cell transplantation

Kimberly Syres, Frank Harrison, Matthew Tadlock, James V. Jester, Jennifer Simpson, Subhojit Roy, Daniel R. Salomon and Stephanie Cherqui

Blood (print ISSN 0006-4971, online ISSN 1528-0020), is published semimonthly by the American Society of Hematology, 1900 M St, NW, Suite 200, Washington DC 20036.

Successful treatment of the murine model of cystinosis using bone marrow cell transplantation

Kimberly Syres,[1] Frank Harrison,[1] Matthew Tadlock,[1] James V. Jester,[2] Jennifer Simpson,[2] Subhojit Roy,[3] Daniel R. Salomon,[1] and Stephanie Cherqui[1]

[1]Department of Molecular and Experimental Medicine, Scripps Research Institute, La Jolla, CA; [2]Department of Ophthalmology, University of California, Irvine, Orange; and [3]Department of Neurosciences, University of California, San Diego, La Jolla

Cystinosis is an autosomal recessive metabolic disease that belongs to the family of lysosomal storage disorders. The defective gene is *CTNS* encoding the lysosomal cystine transporter, cystinosin. Cystine accumulates in every organ in the body and leads to organ damage and dysfunction, including renal defects. Using the murine model for cystinosis, *Ctns*$^{-/-}$ mice, we performed syngeneic bone marrow cell (BMC), hematopoietic stem cell (HSC), and mesenchymal stem cell transplantation. Organ-specific cystine content was reduced by 57% to 94% in all organs tested in the BMC-treated mice. Confocal microscopy and quantitative polymerase chain reaction revealed a large quantity of transplanted BMC in all organs tested, from 5% to 19% of the total cells. Most of these cells were not from the lymphoid lineage but part of the intrinsic structure of the organ. The natural progression of renal dysfunction was prevented, and deposition of corneal cystine crystals was significantly improved in the BMC-treated mice. HSC had the same therapeutic effect as whole BMC. In contrast, mesenchymal stem cell did not integrate efficiently in any organ. This work is a proof of concept for using HSC transplantation as a therapy for cystinosis and highlights the efficiency of this strategy for a chronic, progressive degenerative disease. (Blood. 2009; 114:2542-2552)

Introduction

Cystinosis is an autosomal metabolic hereditary disease characterized clinically by generalized proximal renal tubular dysfunction (Fanconi syndrome) and biochemically by lysosomal accumulation of cystine, which leads to the formation of cystine crystals. Cystinosis belongs to the family of lysosomal storage disorders (LSDs) characterized by the tissue accumulation of incompletely degraded substrates leading to multiple organ dysfunction. The gene underlying cystinosis, *CTNS*, encodes a 7-transmembrane domain protein, cystinosin,[1] a lysosomal cystine transporter.[2,3] Affected persons typically present before 2 years of age with symptoms of severe fluid and electrolyte disturbances (ie, dehydration, vomiting, poor growth, rickets). Without specific treatment, they progress to end-stage renal failure by the end of the first decade[4]; in the United States, cystinosis accounts for approximately 1.4% of children on dialysis and 2% of pediatric kidney transplantations (North American Pediatric Renal Trials and Collaborative Studies, 2008 Annual Report).[5] Cystine accumulation eventually leads to multiorgan dysfunction and patients present with photophobia and blindness, hypothyroidism, hypogonadism, diabetes, myopathy, and central nervous system defects.[6]

Different treatments have been tested for LSD, including enzyme replacement, substrate depletion, and bone marrow transplantation.[7] For cystinosis, substrate depletion with the drug cysteamine reduces the intracellular concentration of cystine. If used early in the disease and in high doses, it can reduce the subsequent progression of renal glomerular damage and other defects.[8] However, the need for frequent dosing and multiple undesirable side effects, such as digestive intolerance and persistent odor, render its chronic administration difficult. Moreover, the proximal renal tubulopathy is not sensitive to cysteamine.

Over the past 2 decades, several reports have established a proof of principle for allogeneic bone marrow stem cell transplantation in several LSDs, including Hurler disease (MPS-I), globoid-cell leukodystrophy (Krabbe disease), and adrenoleukodystrophy.[9,10] Treatment of Hurler patients performed before the age of 2 years has been the most gratifying, and the reconstitution of enzymatic activity is correlated with prolonged survival and, in some cases, normal or near-normal cognitive development and myocardial function.[9,11-13]

Cystinosin is a lysosomal transmembrane protein that cannot be secreted. Therefore, in contrast to Hurler syndrome, the normal enzyme produced by tissue-engrafted cells cannot spread to be recaptured by other cells lacking a functional *Ctns* gene. Therefore, a proof of concept for bone marrow cell transplantation as a therapy for cystinosis is necessary. We used the mouse model, *Ctns*$^{-/-}$ mice, which accumulate cystine and cystine crystals in all organs tested.[14] *Ctns*$^{-/-}$ mice develop ocular changes similar to those observed in affected patients, bone and muscular defects, and behavioral anomalies. *Ctns*$^{-/-}$ mice backcrossed on a C57BL/6 background develop an incomplete proximal tubulopathy and renal failure by 15 months of age.[15]

Here we report that syngeneic bone marrow transplantation from wild-type (WT) donors into *Ctns*$^{-/-}$ mice successfully protected these animals from the progression of the kidney tissue injury and corneal cystine deposition that represent 2 of the major clinical problems faced by children and young adults with this genetic disorder. There was significant engraftment of donor bone

Submitted March 30, 2009; accepted May 30, 2009. Prepublished online as *Blood* First Edition paper, June 8, 2009; DOI 10.1182/blood-2009-03-213934.

The publication costs of this article were defrayed in part by page charge payment. Therefore, and solely to indicate this fact, this article is hereby marked "advertisement" in accordance with 18 USC section 1734.

marrow–derived cells in every tissue compartment tested as determined by confocal microscopy and quantitative polymerase chain reaction (PCR). Mechanistically, only engraftment of bone marrow cells producing a functional *Ctns* was able to reverse the disease process. Second, quantitative expression of functional *Ctns* and tissue colonization by bone marrow cell (BMC)–derived cells measured by luciferase imaging in these animals correlated in each tissue compartment with reduction of cystine levels of 57% to 94% as measured by tandem mass spectrometry.

Methods

Mice

C57BL/6 *Ctns*$^{-/-}$ mice were provided by Dr C. Antignac (Inserm U574) and bred continuously at the Scripps Research Institute. Transgenic mice constitutively expressing green fluorescent protein (GFP; C57BL/6-Tg(ACTB-EGFP)1Osb/J) were obtained from The Jackson Laboratory. Transgenic mice constitutively expressing firefly luciferase were provided by Dr M. Geusz (Bowling Green State University). All protocols were approved by the Association for Assessment and Accreditation of Laboratory Animal Care–Accredited Institutional Animal Care and Use Committee of the Scripps Research Institute.

BMC and HSC isolation, MSC generation, and cell transplantation

BMCs were flushed from the long bones of 6- to 8-week-old mice and transplanted without further culture or processing. Sca1^{+} bone marrow progenitors (hematopoietic stem cell [HSC]) were sorted using anti-Sca1 antibody conjugated to mini-magnetic beads (Miltenyi Biotec). Mesenchymal stem cells (MSCs) were generated as previously described.[16] Briefly, BMCs from GFP-transgenic mice were plated at a density of 5×10^6 cells/mL in Dulbecco modified Eagle medium-low glucose-containing 10% fetal bovine serum (HyClone Laboratories), 3.7 g/L sodium bicarbonate, 10 mM N-2-hydroxyethylpiperazine-N′-2-ethanesulfonic acid, and 100 U/mL penicillin/streptamycin (Invitrogen). Cultures were plated 3.5 mL per well of 6-well tissue culture dishes and were kept at 37°C 5% CO_2. The media was changed 72 hours after plating and then every 3 days. When cultures reached confluence, cells were split at a 1:2 ratio. At each passage, cells were stained with phycoerythrin-conjugated anti-CD45, CD44 (BD Biosciences Pharmingen), CD34, CD31 (Invitrogen), CD105 (R&D Systems), and CD90.2 (eBioscience) antibodies and analyzed by flow cytometry to determine the phenotype of the cells. Cells were injected via the tail vein. The mice were lethally (cesium radiation, 8 Gy) for BMCs and HSCs, or sublethally (3.6 Gy) for MSCs, irradiated the day preceding the injection. To analyze engraftment, fresh blood was treated with red blood cell lysis buffer (eBioscience) and subjected to flow cytometry to quantify GFP-positive cells. Lineage-specific staining and flow cytometry allowed determination of the hematopoietic chimerism for T cells (Cy-Chrome–conjugated anti-CD3ϵ; BD Biosciences Pharmingen), B cells (phycoerythrin-conjugated anti-CD19; BioLegend), and macrophages (phycoerythrin-conjugated MAC3; BD Biosciences Pharmingen). Appropriate isotype controls were used for each.

Blood and urine analysis

Serum was obtained by eye bleeds, and 24-hour urine collections were done in metabolic cages. Serum and urine phosphate levels as well as serum creatinine, urea, and alkaline phosphatase were estimated using colorimetric assays according to the manufacturer's recommendations (BioAssay Systems). Protein levels in urine were measured using Pierce BCA Protein Assay Kit.

Quantitative RT-PCR

RNA was isolated from explanted tissues by homogenization in 750 μL TRIzol LS Reagent (Invitrogen). Phase separation was performed with the addition of 200 μL chloroform followed by centrifugation. After removal of the aqueous phase, RNA was recovered by precipitation with isopropyl alcohol. RNA was purified using the RNeasy mini-protocol for RNA cleanup, including DNase treatment on column (QIAGEN). A total of 1 μg RNA for each tissue was reverse-transcribed (RT) using iScript cDNA Synthesis Kit (Bio-Rad). For peripheral blood engraftment determination, 300 μL mouse whole blood was collected by cardiac puncture and placed in 600-μL PAXgene blood RNA preservative solution obtained from PAXgene Blood RNA Tubes (PreAnalytix QIAGEN) followed by RNA purification using the PAXgene Blood RNA Kit (PreAnalytix QIAGEN).

Ctns-specific quantitative PCR was performed using 2 μL cDNA and 2× Universal TaqMan Master Mix (Roche Diagnostics), *Ctns* primer mix (in *Ctns* exon 8: *Ctns* oligo 1: TTGTGGCTGCAGTCGGTATC, *Ctns* oligo 2: AGCTTGATGTAGGAGAAGCAGAAGA, and *Ctns* probe: CACATGGCTCCAGTTC (Applied Biosystems) and 18s primer mix (Applied Biosystems) on an Applied Biosystems 7900 HT.

Immunofluorescence analysis

Tissues were fixed in formaldehyde 5%, equilibrated in sucrose 20% overnight, and frozen in Tissue-Tek Optimal Cutting Temperature buffer at −80°C (Sakura Finetek). Twelve- to 20-μm-thick sections were cut and blocked with 1% bovine serum albumin, 10% donkey serum in phosphate-buffered saline. The blocking buffer was then diluted 1:5 in phosphate-buffered saline and antibody added in the dilutions denoted below and incubated with sections at room temperature for 1 hour; the lectins were incubated for 2 hours. Each tissue was stained with 4,6-diamidino-2-phenylindole (DAPI) and Bodipy-phalloidin (1:500 dilutions for 30 minutes; Invitrogen) or Cy5-conjugated anti-F4/80 antibody (1:50 dilution; Serotec) and biotinylated anti–mouse CD45 antibody (1:500 dilution; BD Biosciences Pharmingen) followed by Alexa 594–conjugated streptavidin (1:100 dilution; Invitrogen). Kidney sections were stained with rhodamine-conjugated *Dolichos biflorus* agglutinin (1:100 dilution), rhodamine-conjugated *Ricinus communis* agglutinin I (1:250 dilution), biotinylated Lotus tetragonolobus lectin (1:100 dilution; Vector Laboratories) followed by Alexa 594–conjugated streptavidin, and rabbit anti–human von Willebrand factor (VWF, 1:200 dilution; Dako) followed by donkey anti–rabbit IgG conjugated with Cy5 (1:100 dilution). Brain sections were stained with a mouse pan antiaxonal microfilament antibody (1:250 dilution; Covance) and a mouse antiglial fibrillary acidic protein (1:500 dilution; Millipore), followed by a donkey anti–mouse IgG conjugated with Alexa 594 (1:100 dilution; Jackson ImmunoResearch Laboratories). Images were acquired using a Rainbow Radiance 2100 Laser Scanning Confocal system attached to a Nikon TE2000-U inverted microscope (Bio-Rad–Carl Zeiss). All images were 8-bit optical image slices (0.5-μm interval step slices) acquired using LaserSharp 2000 software. Images were then analyzed with IMARIS 4.2 imaging software (Bitplane Scientific Solutions) to generate 3-dimensional reconstruction series of optical slices (Z-stacks).

Tandem scanning reflectance confocal microscopy

Reflectance confocal microscopy was performed on enucleated mouse eyes of various ages. Examinations were performed using a Tandem Scanning Confocal Microscope (Tandem Scanning Corporation) with a 24× surface-contact objective (numerical aperture, 0.6; working distance, 1.5 mm), Oriel 18 011 Encoder Mike Controller (Oriel Corp) for focal plane control, and Dage MTI VE-1000 camera (Dage MTI). One drop of artificial tear solution was placed on the tip of the objective as a coupling gel. All camera settings were kept constant throughout the experiment. For each examination, repeated through-focus datasets were obtained from the peripheral cornea and limbal region to identify cystine crystals and GFP-positive cells.

Cystine content measurement

Explanted tissues were grounded in 750 μL N-ethylmaleimide (Fluka Biochemika) at 650 μg/mL for cystine measurements. The proteins were precipitated using 15% 5-sulfosalicylic acid dihydrate (Fluka Biochemika), resuspended in NaOH 0.1 N, and measured using the Pierce BCA protein assay kit. The cystine-containing supernatants were sent to the University of

Table 1. Serum and urine analyses for renal function (n = 12 per group)

	Wild-type controls	Ctns$^{-/-}$ controls	WT BMCs	Ctns$^{-/-}$ BMCs	WT MSCs
Serum					
Creatinine, mg/dL	0.34 ± 0.06	0.49 ± 0.30*†	0.35 ± 0.07	0.43 ± 0.10*†	0.38 ± 0.11
Creatinine clearance, μL/min	79.40 ± 74.24	32.28 ± 42.58	65.65 ± 72.34	43.04 ± 34.46	85.35 ± 64.60
Urea, mg/dL	36.54 ± 1.55	56.92 ± 18.41*†	23.83 ± 19.62	74.95 ± 17.32*†	41.98 ± 4.85†
Phosphate, mg/dL	18.31 ± 3.06	23.09 ± 4.70†	10.95 ± 6.82	10.57 ± 7.53	11.86 ± 6.35
Alkaline phophatase, IU/L	60.54 ± 23.57	67.35 ± 26.75	75.77 ± 21.10	67.76 ± 18.10	55.73 ± 16.20
Urine					
Phosphate, μmol/24 h	3.50 ± 2.29	11.00 ± 4.90*†	3.75 ± 2.35	2.70 ± 2.87	5.11 ± 3.29
Protein, mg/24 h	10.16 ± 6.21	17.28 ± 8.45	9.37 ± 6.91	8.35 ± 4.35	11.43 ± 7.08

Wild-type controls indicate nontreated WT C57BL/6 mice; Ctns$^{-/-}$ controls, nontreated C57BL/6 *Ctns*$^{-/-}$ mice; WT BMCs, *Ctns*$^{-/-}$ mice treated with WT BMCs; Ctns$^{-/-}$ BMCs, *Ctns*$^{-/-}$ mice treated with Ctns$^{-/-}$ BMCs; and WT MSCs, *Ctns*$^{-/-}$ mice treated with WT MSCs.

*$P < .05$ vs wild-type mice.

†$P < .05$ vs Ctns$^{-/-}$ WT BMCs.

California, San Diego Biochemical Genetics laboratory for measurements by mass spectrometry.

Live animal luciferase imaging

Mice transplanted with BMCs isolated from luciferase transgenic mice were measured at 2, 3, and 4 months after transplantation using the IVIS Imaging System 200 Series (Caliper Life Sciences). First, the mice were anesthetized, and 75 μL luciferin (30 mg/mL; Caliper Life Sciences) was injected intraperitoneally 10 minutes before the observation. Quantitative signal analysis was done using the Living Image 2.5 software (Caliper Life Sciences).

Statistics

We expressed data as arithmetic mean plus or minus SD and performed statistical analysis using one-tailed *t* tests as the samples were large enough and normally distributed. A *P* value less than .05 was considered statistically significant. Corneal cystine crystals were recorded as a simple present or absent result, and statistics were done by χ^2 analysis.

Results

Freshly harvested BMCs were used for transplantation. MSCs were prepared by culture following Dr Mereilles' protocol[16] and used at passage 20. The phenotype of the MSCs was tested and confirmed by flow cytometry at the time of transplantation: positive for CD44, CD90.2, and CD105 and negative for CD45, CD31, and CD34 (data not shown). We transplanted 2×10^7 WT C57BL/6 BMCs or 10^6 MSC in lethally or sublethally irradiated *Ctns*$^{-/-}$ mice, respectively. As controls, we transplanted 2×10^7 Ctns$^{-/-}$ BMCs into lethally irradiated *Ctns*$^{-/-}$ mice. The groups were WT mice, untreated *Ctns*$^{-/-}$ mice, WT BMC-treated *Ctns*$^{-/-}$ mice, and Ctns$^{-/-}$ BMC-treated *Ctns*$^{-/-}$ mice. Within each group, the animals were age-matched littermates and a mix of males and females. Mice were between 2 and 4 months of age when transplanted and killed 4 months later for analysis. These experiments were repeated 3 times (n = 5 mice) for a total of 15 mice per group. Three mice per group were killed 2 months after injection to determine whether tissue integration was increasing with time. To allow tracking of cells by confocal microcopy, we transplanted 4 *Ctns*$^{-/-}$ mice and 4 WT controls with BMCs from GFP-transgenic mice. All transplanted MSCs were from GFP-transgenic mice.

Cell engraftment was determined in peripheral blood by quantifying either GFP-positive cells by flow cytometry or by quantitative RT-PCR for the WT *Ctns* gene. Engraftment ranged from 5% to 90% in mice transplanted with WT BMCs and 3% to 6% in mice transplanted with MSCs. The survival rate for BMC-transplanted mice after lethal irradiation was 93%, and all the surviving mice exhibited benefits. The contribution of donor-derived cells within each lineage was determined for 5 mice transplanted with GFP-transgenic BMCs and for which the peripheral blood engraftment was 72% plus or minus 17%; 86% plus or minus 7% were GFP-positive T lymphocytes, 69% plus or minus 11% were B lymphocytes, and 45% plus or minus 21% were macrophages.

Kidney

In all the experimental groups described in the first paragraph of "Results," renal function was assessed by measuring creatinine, urea, alkaline phosphatase, and phosphate levels in the serum and creatinine clearance, protein, and phosphate in 24-hour urine collections. Serum creatinine and urea of *Ctns*$^{-/-}$ mice transplanted with WT BMCs were significantly better than control *Ctns*$^{-/-}$ mice and *Ctns*$^{-/-}$ mice transplanted with Ctns$^{-/-}$ BMCs (Table 1). Moreover, kidney function of mice transplanted with WT BMCs was not significantly different from WT controls. Serum urea was increased in *Ctns*$^{-/-}$ mice treated with WT MSC compared with *Ctns*$^{-/-}$ mice treated with WT BMCs, but the creatinine levels were normal.

Kidney sections for each group of mice defined in the first paragraph were analyzed by confocal microscopy for the presence of GFP-positive cells. We did not observe any GFP-positive cells in *Ctns*$^{-/-}$ mice treated with Ctns$^{-/-}$ BMCs (Figure 1A-B) as a negative control for imaging of GFP in the experimental groups. Only few GFP-positive cells were observed in mice transplanted with GFP MSCs (< 5 cells per section; data not shown). WT mice treated with WT BMCs isolated from GFP-transgenic mice (GFP BMCs) also revealed very few GFP-positive cells in the kidney (Figure 1C-D). In contrast, *Ctns*$^{-/-}$ mice transplanted with GFP BMCs showed abundant BMC-derived cells (Figure 1E-F).

Most of the GFP-positive cells in *Ctns*$^{-/-}$ mice transplanted with GFP BMCs were interstitial, but only a few were of lymphoid or macrophage lineage as defined by CD45 and F4/80 staining, respectively (Figure 2A). GFP-positive cells colocalized with proximal and distal tubular cells and some were in glomeruli (Figure 2B-D). Finally, GFP-positive cells were colocalized to tubular and glomerular basement membranes or with endothelial cells (Figure 2E-F).

Eye and brain

One eye per mouse was analyzed by confocal microscopy for the presence or absence of corneal cystine crystals and GFP-positive

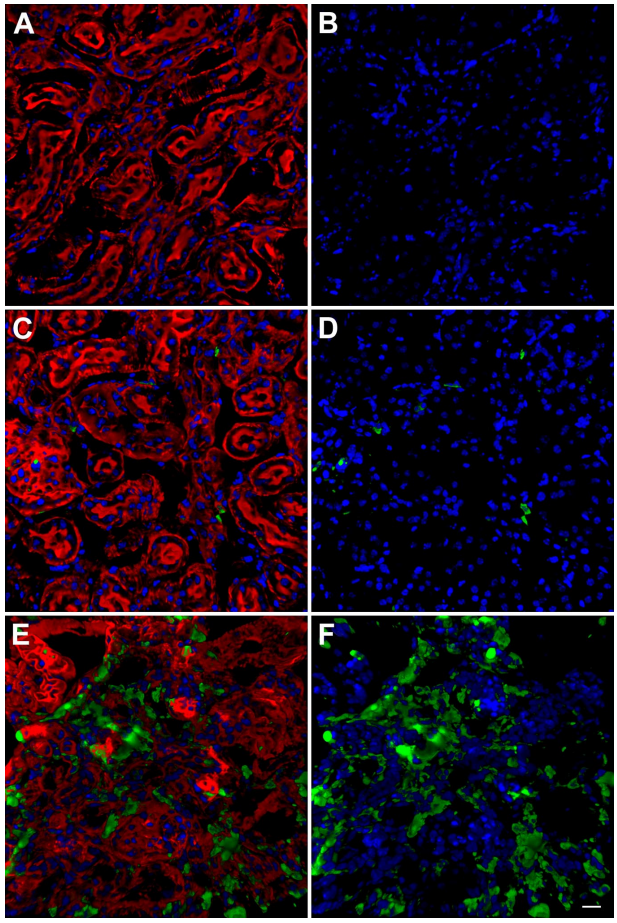

Figure 1. Representative images of Z-series confocal microscopy of kidneys. Transplanted, BMC-derived, GFP-positive cells are seen in green. (A,C,E) F-actin intermediate filament staining by Bodipy-phalloidin (red) and nuclei staining by DAPI (blue). (B,D,F) Same picture without Bodipy-phalloidin to better observe the GFP-positive cells. (A-B) Kidney section of *Ctns*$^{-/-}$ mice treated with Ctns$^{-/-}$ BMC; no GFP-positive cells are observed establishing the threshold for GFP detection. These instrument settings were saved and used for all the subsequent imaging. (C-D) Representative kidney section of WT mice transplanted with GFP BMCs. Few GFP-positive cells are observed. (E-F) Kidney section of *Ctns*$^{-/-}$ mice transplanted with GFP BMCs. Abundant GFP-positive BMC-derived cells are evident. Scale bar represents 20 μm (40×/1.3 NA oil objective).

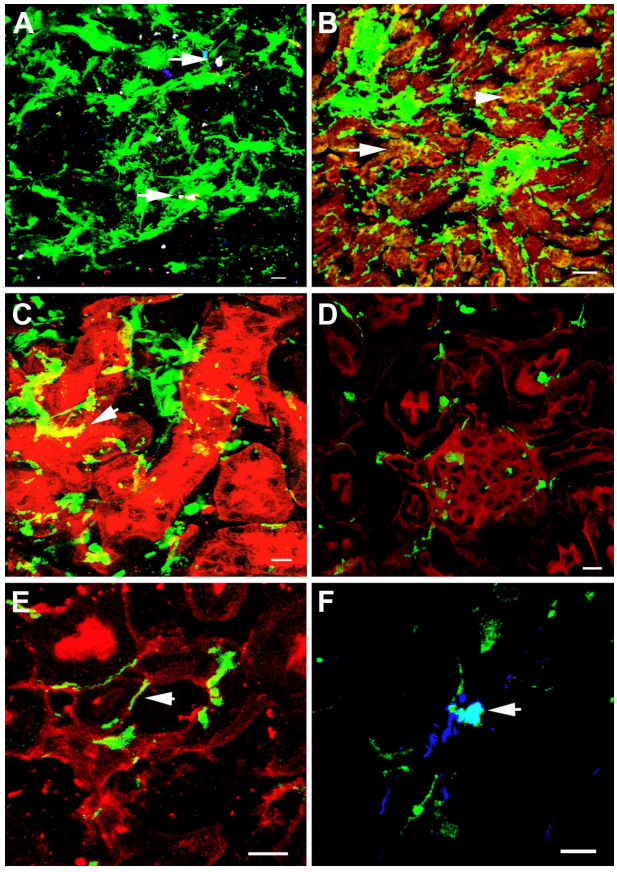

Figure 2. Representative Z-series confocal microscopy pictures of WT BMC-treated kidneys to demonstrate cell phenotypes. Transplanted, BMC-derived, GFP-positive cells are seen in green. (A) F4/80-positive macrophages are stained in blue, and CD45-positive leukocyte lineage cells are stained in red. Few GFP-positive cells are macrophages (white, arrows). (B) Distal tubular staining by *D biflorus* agglutinin (red). Some GFP-positive cells are colocalized with distal tubular cells (yellow, arrows). (C) Proximal tubular staining by *Lotus tetragonolobus* lectin (red). Some GFP-positive cells are colocalized with proximal tubular cells (yellow, arrow). (D) F-actin intermediate filament staining by Bodipy-phalloidin (red). Some GFP-positive cells are found in the glomeruli. (E) Tubular basement membrane staining by Ricinus communis agglutinin I (red). Some GFP-positive cells colocalize with the basal membranes (arrow). (F) Endothelial cell staining with anti-VWF antibody (blue). Some GFP-positive cells are colocalized with endothelial cells (white, arrow). Scale bars represent 10 μm (60×/1.4 NA oil objective), except for panel B, in which scale bar represents 50 μm (20×/0.75 NA air objective).

cells. Cystine crystals were detected only in mice more than 7 months of age. Of 7 Ctns$^{-/-}$ BMC-treated *Ctns*$^{-/-}$ mice, 6 presented cystine crystals (Figure 3D). However, in 7 age-matched WT BMC-treated mice, only 3 had cystine crystals in the cornea (treated vs nontreated, $P < .05$, χ^2). GFP-positive cells were observed in the peripheral cornea, localized to the corneal stroma (Figure 3A) and adjacent to the basal cells of the corneal epithelium (Figure 3B). GFP-positive cells generally had a dendritic (Langerhans) cell–like morphology. At the vascularized limbus, a heavy perivascular infiltrate was also observed (Figure 3C). No GFP-positive cells were observed in mice transplanted with GFP MSCs.

We analyzed the brains by confocal microscopy. GFP-positive cells were observed in all brain regions. Most of these cells were associated with blood vessels. Some were small, round, and were associated with delicate intraparenchymal vessels. These cells were particularly prominent in the basal ganglia and thalamus and were found within the blood vessel lumens. Some also appeared to be attached to the endothelium, and some large, flattened GFP-positive cells were also seen. These cells with an endothelial-like morphology were further characterized by double immunofluorescence staining; they were positive for smooth muscle or endothelial markers (Figure 3E-F). A few cells also colocalized with macrophage and glial markers (Figure 3G-H). No GFP-positive cells were observed in mice transplanted with MSCs.

Muscle, spleen, liver, and heart

Mice transplanted with MSCs present with very few GFP-positive cells in muscle, spleen, liver, and heart. In contrast, mice that received BMCs had a large quantity of transplanted BMC-derived cells in all these tissues. In the muscle, most of the GFP-positive cells were nonlymphoid lineage interstitial cells. However, the observation of some GFP-positive muscle cells indicated a subset of transplanted BMC-derived cells probably fused with muscle fibers (Figure 4A-C). In the heart, the GFP-positive cells were interstitial (data not shown). In the liver, most of the GFP-positive cells were Kupffer cells, colocalizing with macrophages (F4/80) and leukocyte lineage cells (CD45$^+$; data not shown). Spleen demonstrated the most GFP-positive cells of any tissue. Surprisingly, the majority were not of the lymphoid lineage (CD45$^-$ and

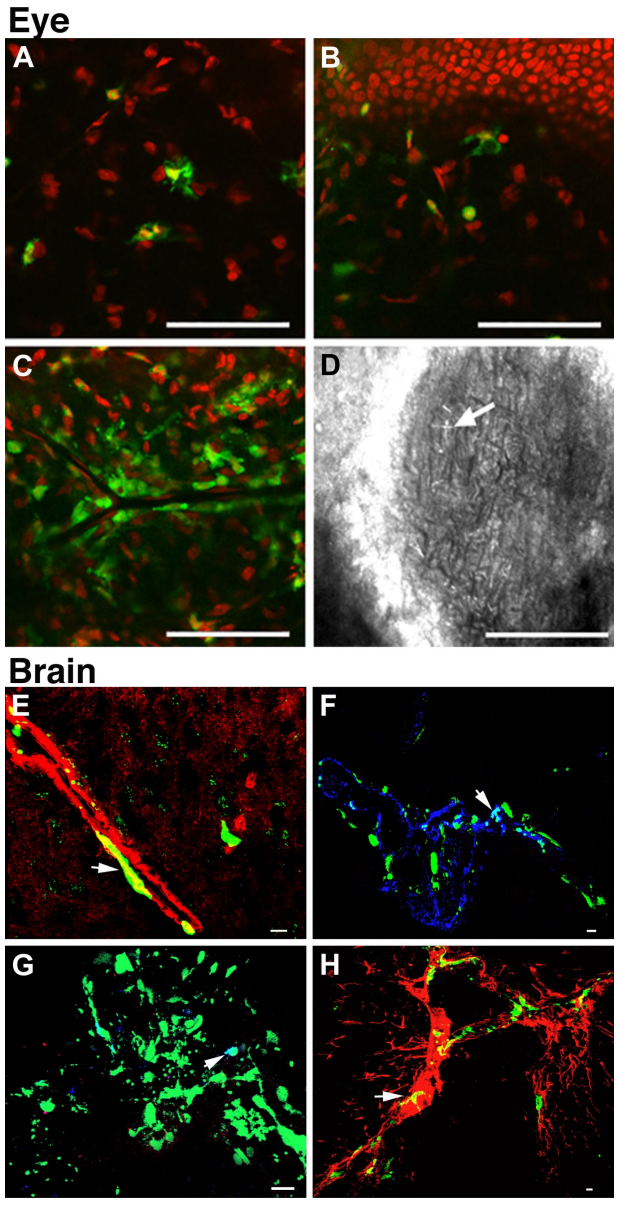

Figure 3. Representative Z-series confocal microscopy pictures of the eyes and brains of mice treated with WT BMCs. Transplanted, BMC-derived, GFP-positive cells are seen in green. (A-D) Eye. Bodipy-phalloidin is seen in red. Scale bars represent 50 μm (24×/0.6 NA air objective). GFP-positive cells were observed in the corneal stroma (A) and adjacent to the basal cells of the corneal epithelium (B). Heavy perivascular infiltrates around the limbus were also observed (C). Corneal cystine crystals (D, arrow). (E-H) Brain. Scale bars represent 10 μm (E: 60×/1.4 NA oil objective; F-H: 40×/1.3 NA oil objective). The majority of the GFP-positive cells were observed in association with blood vessels. Small round cells were observed in the lumen, many appearing to be attached to the endothelium. Large flat cells were either fused with or differentiated into smooth muscle cells colocalizing with F-actin seen in red (E, yellow, arrow) or endothelial cells colocalizing with VWF seen in blue (F, white, arrow). A few GFP-positive cells were macrophages (G, white, arrow). Some were glial cells colocalizing with glial fibrillary acidic protein staining seen in red (H, yellow, arrow).

F4/80$^-$), but they were VWF- and F-actin–positive, consistent with splenic reticuloendothelial cells (Figure 4D-F).

Cystine content, tissue *Ctns* expression, and dynamics

Cystine contents of brain, eye, heart, kidney, liver, muscle, and spleen were measured at 2 months (n = 3/group) and 4 months (n = 12/group; Table 2; Figure 5). Cystine levels increased in all tissues in Ctns$^{-/-}$ BMC-treated mice as a function of time. In MSC-treated mice, a decrease in cystine level was significant only in heart at 2 months, but levels increased at 4 months. In contrast, as early as 2 months, Ctns$^{-/-}$ mice transplanted with WT BMCs demonstrated a decrease in cystine content compared with Ctns$^{-/-}$ BMC-treated mice. This cystine content decrease was observed in all the tissues, except the kidney, but was only statistically significant in the spleen and liver. By 4 months, cystine levels were significantly less in WT BMC-treated mice in all the tissues tested, ranging from a 57% decrease in the brain to 94% in the liver.

Quantitative RT-PCR with *Ctns*-specific primers was performed in the same tissues at 2 and 4 months after transplantation (Table 3). No *Ctns* expression was detected in Ctns$^{-/-}$ BMC-treated mice. The results confirmed the high level of engraftment observed for WT BMCs and the low engraftment of MSC-derived cells. Thus, *Ctns* expression decreased in MSC-treated mice in all tissues, except spleen between 2 and 4 months. *Ctns* expression was highest in mice treated with WT BMCs in the spleen, confirming the confocal microscopy data (Figure 4). To show the changes in time, we normalized the quantitative RT-PCR values for *Ctns* expression at 2 and 4 months by taking the ratio of the WT values to the Ctns$^{-/-}$ mice transplanted with WT BMCs. These results demonstrate that *Ctns* expression increased between 2 and 4 months after injection in every tissue (Figure 6B). By 4 months, *Ctns* expression ranged between 5.4% of the total *Ctns* expressed in WT mice in muscle to 19.3% in spleen.

Finally, to follow the fate of transplanted BMCs expressing a functional *Ctns* gene in live animals as a function of time, we transplanted 10 *Ctns*$^{-/-}$ mice and 5 WT controls with BMCs isolated from luciferase-transgenic mice. The mice were imaged at 2, 3, and 4 months after transplantation, and luciferase expression was quantitatively measured. At each time point, 4 pictures for each mouse were taken, representing the ventral, dorsal, left, and right side views. Figure 6A is a representative ventral view picture of the same *Ctns*$^{-/-}$ and WT mice at the 3 different time points. The significant increase of luciferase intensity and tissue area with time is clearly evident in the *Ctns*$^{-/-}$ mouse and correlates with our evidence for the engraftment of BMC-derived cells in multiple tissues. In contrast, in WT mice, the luciferase expression remains minimal over time.

HSCs

We showed that whole BMCs efficiently integrated in multiple organs, resulting in significant decreases of cystine content in these tissues. BMC is a heterogeneous mixture of cells that contains a small number of HSCs. For the purpose of a clinical application, we need to know if whole bone marrow is necessary to achieve our objectives or if similar results can be obtained with purified HSCs only. We lethally irradiated and transplanted 10 2-month-old *Ctns*$^{-/-}$ mice with Sca1$^+$ HSCs isolated from GFP-transgenic mice. These were all killed at 4 months after transplantation for analysis. All these mice had high levels of peripheral blood engraftment of transplanted cells, ranging from 73% to 94% (hematopoietic lineage chimerism: 95% ± 3% for T lymphocytes, 65% ± 14% for B lymphocytes, and 50% ± 14% for macrophages). Controls included nontreated *Ctns*$^{-/-}$ mice and WT animals at the same ages. Mice transplanted with Sca1$^+$ GFP HSCs showed abundant GFP-positive cells within all the tissues tested by confocal microscopy (data not shown). Quantitative RT-PCR with *Ctns*-specific primers showed a high level of engraftment of Sca1$^+$ HSC-derived cells in all the tissues tested of *Ctns*$^{-/-}$-treated mice (Table 4). The relative expression of *Ctns* gene in HSC-treated

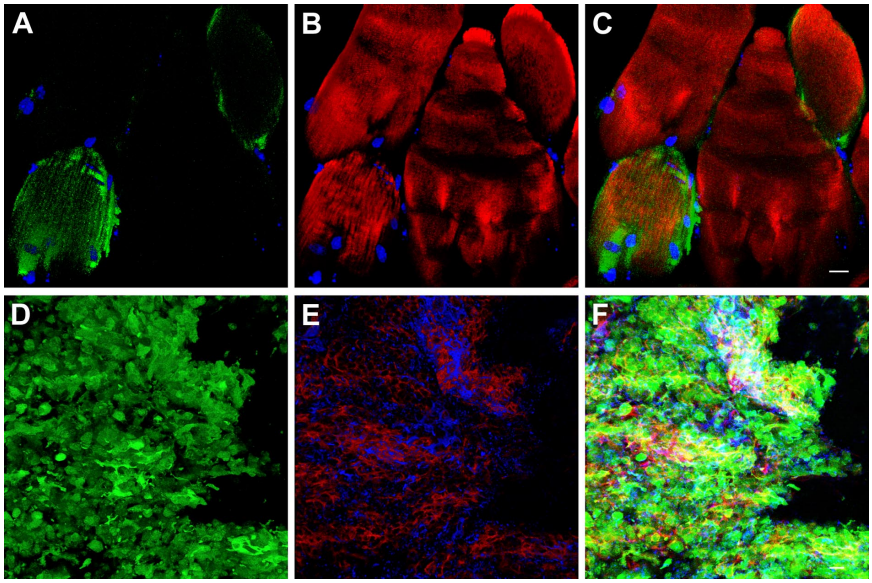

Figure 4. Representative Z-series confocal microscopy pictures of the muscle and spleen of mice treated with WT BMCs. Transplanted, BMC-derived, GFP-positive cells are seen in green (A,D). F-actin intermediate filament staining by Bodipy-phalloidin is seen in red (B,E), and colocalization of both stains is shown in the last panels (C,F). Muscle (A-C). Nuclei stained by DAPI are blue. Some GFP-positive cells are interstitial, and some are differentiated or fused with muscle fibers as shown by the colocalization of GFP-positive with muscle fibers (C). Spleen (D-F). Most of the GFP-positive cells in the spleen are part of the reticuloendothelium as determined by colocalization with VWF (blue) and F-actin staining (F). Scale bars represent 10 μm (A-C: 60×/1.4 NA oil objective; D-F: 40×/1.3 NA oil objective).

Ctns$^{-/-}$ mice compared with WT was expressed in percentages, from 2.1% in the brain to 77.5% in the spleen. Tissue cystine levels were also significantly decreased in HSC-treated *Ctns*$^{-/-}$ mice compared with nontreated *Ctns*$^{-/-}$ mice controls, from a 43.5% decrease in the kidney to 93.2% in the liver (Table 5). The renal function of HSC-transplanted *Ctns*$^{-/-}$ mice was also normal as defined by serum urea and creatinine levels (data not shown).

Discussion

Cystinosis is a hereditary, autosomal recessive genetic disease of childhood that results in progressive cellular injury to many different tissues because of the accumulation of cystine in lysosomes. The introduction of oral cysteamine therapy in 1994[17] has significantly improved the quality of life of patients with cystinosis and has reduced the rate of progression of tissue injury.[8] However, curative therapy for hereditary genetic diseases, such as the LSDs, requires the addition of the gene to many cells, typically in multiple tissue compartments, or the progressive replacement of injured and dying cells by cells expressing the functional version of the gene. Recently, an attempt to deliver the *CTNS* gene to the liver of *Ctns*$^{-/-}$ mice with an adenoviral vector demonstrated a limited decrease in cystine content but only with young animals and very low expression of the transgene.[15] Stem cell transplantation represents an alternative strategy, and there has been some success in other LSDs, particularly with Hurler disease.[9,10] Here we report the effective use of both BMC and HSC transplantation to prevent the development and progression of kidney injury and dysfunction in *Ctns*$^{-/-}$ mice. We also demonstrate the engraftment of BMC- and HSC-derived cells in multiple tissue compartments known to reflect clinical disease in the course of cystinosis and document significant reductions in tissue cystine content in all these compartments.

The therapeutic potential of stem cell transplantation for renal disorders is controversial.[18] Some authors showed that BMCs can migrate to a damaged kidney and give rise to proximal tubular cells,[19] podocytes,[20] and other glomerular cells,[21] and reverse renal dysfunction[19] or treat a genetic kidney disease, such as Alport syndrome.[22] However, other authors deny the possibility that renal cells can derive from transplanted bone marrow. One study concluded that intrarenal stem cells, but not bone marrow-derived cells, are responsible for the regeneration of kidney tissue after ischemic injury, and injection of BMCs does not make any significant contribution to functional or structural recovery.[23] A second study showed that 99% of the BMC-derived cells engrafted in the kidney were leukocytes.[24] In the mouse model of cystinosis, our data demonstrate that, in the context of chronic and progressive renal damage, BMC-derived cells can efficiently engraft in the kidney tissue compartment, lead to a significant decrease in cystine content, and prevent progression of kidney dysfunction. Indeed, 4 months after transplantation, 13% of the total renal cells as determined by quantitative PCR (Figure 6B) were derived from the

Table 2. Cystine content in different tissues of treated and control mice at 2 and 4 months after transplantation

	2 months (n = 3 animals per group)				4 months (n = 12 animals per group)			
Tissue	Wild-type controls	Ctns$^{-/-}$ BMCs	WT BMCs	WT MSCs	Wild-type controls	Ctns$^{-/-}$ BMCs	WT BMCs	WT MSCs
Brain	0.02 ± 0.00	0.70 ± 0.15	0.61 ± 0.29	0.75 ± 0.28	0.02 ± 0.00	1.38 ± 0.45	0.59 ± 0.32*	0.62 ± 0.39*
Eye	0.07 ± 0.20	20 ± 11	18 ± 11	27 ± 4	0.1 ± 0.02	45 ± 12	13 ± 8*	36 ± 9
Heart	0.17 ± 0.10	25 ± 7	23 ± 16	10 ± 1*	0.08 ± 0.10	61 ± 15	11 ± 8*	25 ± 9*
Kidney	0.18 ± 0.05	76 ± 16	135 ± 12	45 ± 24	0.25 ± 0.06	116 ± 63	35 ± 34*	59 ± 34*
Liver	0.02 ± 0.01	57 ± 3	6 ± 0.2*	62 ± 23	0.02 ± 0.02	62 ± 19	3 ± 1*	51 ± 15
Muscle	0.23 ± 0.13	17 ± 7	15 ± 2	10 ± 0.7	0.07 ± 0.20	30 ± 11	10 ± 6*	22 ± 4
Spleen	0.06 ± 0.04	91 ± 39	38 ± 5*	124 ± 35	0.12 ± 0.03	160 ± 50	21 ± 19*	95 ± 17*

Cystine content is stated in nmol half-cystine/mg protein.
*$P < .05$ versus mice treated with Ctns$^{-/-}$ BMCs.

A

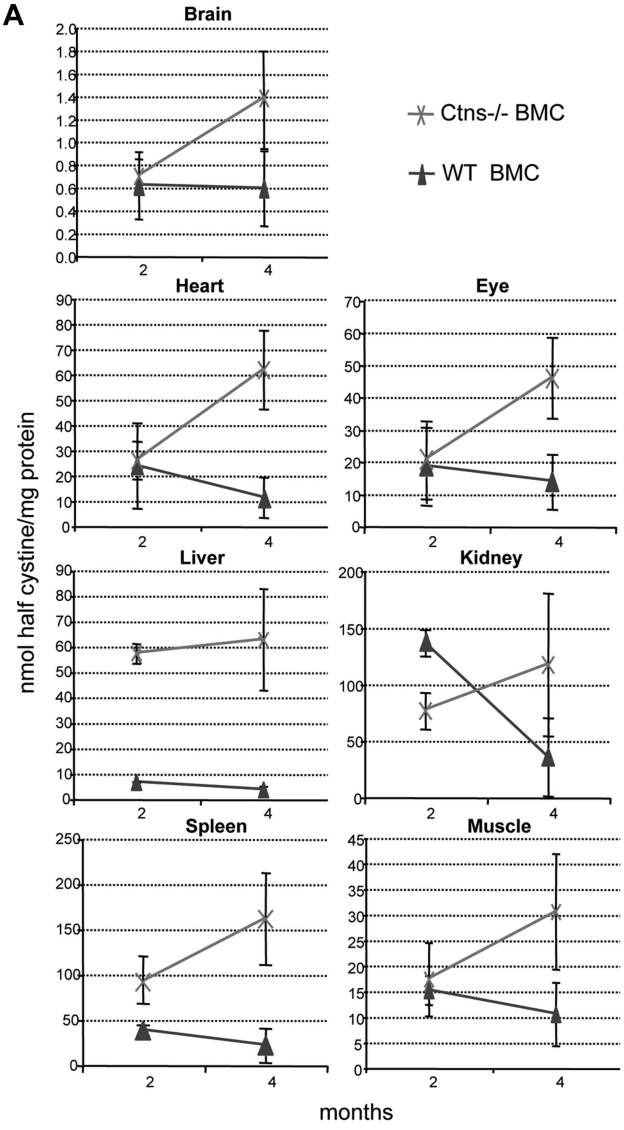

B

	Percent decrease in cystine*	
	2 months	4 months
Brain	11.6	57.3
Eye	9.5	70.4
Heart	8.4	81.9
Kidney	-35.7	70
Liver	88.4	94.4
Muscle	12.2	65.6
Spleen	58.2	86.8

*Percent decrease in cystine content in *Ctns*$^{-/-}$ mice treated with WT BMC compared to *Ctns*$^{-/-}$ mice treated with Ctns$^{-/-}$ BMC.

Figure 5. Tissue cystine content in *Ctns*$^{-/-}$ mice treated with WT BMCs compared with *Ctns*$^{-/-}$ mice treated with Ctns$^{-/-}$ BMCs. (A) Cystine content at 2 and 4 months in *Ctns*$^{-/-}$ mice. Cystine levels increase with time after transplantation of Ctns$^{-/-}$ BMCs (×). In contrast, cystine content decreases in time after therapy with WT BMCs (▲). (B) Table of percentage decrease in cystine content of *Ctns*$^{-/-}$ mice treated with WT BMCs compared with *Ctns*$^{-/-}$ mice treated with Ctns$^{-/-}$ BMCs.

infused WT BMCs expressing functional *Ctns*. These BMC-derived cells were predominately nonlymphoid lineage interstitial cells but also colocalized with distal and proximal tubular, glomerular, and endothelial cells. Moreover, the treated mice exhibited normal serum urea and creatinine levels in contrast to control mice treated with Ctns$^{-/-}$ BMCs. The renal disease in children with cystinosis starts as a proximal tubulopathy before 1 year of age and then evolves to a progressive loss of glomerular function.[6] Cystine crystals are not abundant in the kidney and are mostly observed in interstitial cells, occasionally in glomerular cells, and rarely in

Table 3. *Ctns* expression in different tissues of treated and control mice at 2 and 4 months after transplantation

	2 months (n = 3 animals per group)				4 months (n = 12 animals per group)			
Tissue	Wild-type controls	Ctns$^{-/-}$ BMC	WT BMCs	WT MSCs	Wild-type controls	Ctns$^{-/-}$ BMCs	WT BMCs	WT MSCs
Brain	40 352 ± 41 063	ND	694 ± 842	2 ± 2	8362 ± 3814	ND	520 ± 151	1 ± 1
Eye	124 553 ± 17 116	ND	14 722 ± 20 816	12 ± 13	52 942 ± 35 772	ND	8226 ± 3361	2 ± 2
Heart	44 510 ± 15 675	ND	3865 ± 5415	2 ± 1	27 089 ± 13 649	ND	3359 ± 2761	1 ± 1
Kidney	304 504 ± 95 560	ND	6569 ± 1749	31 ± 54	47 709 ± 26 694	ND	7071 ± 10 917	3 ± 6
Liver	38 616 ± 32 898	ND	674 ± 319	15 ± 23	180 281 ± 15 749	ND	19 201 ± 12 787	1 ± 0
Muscle	36 233 ± 15 457	ND	342 ± 119	ND	28 148 ± 12 428	ND	1617 ± 1223	3 ± 4
Spleen	185 567 ± 24 855	ND	1375 ± 968	3 ± 3	136 147 ± 11 703	ND	32 555 ± 14 730	6 ± 10

Relative expression of *Ctns* as18S-normalized fold changes is shown.
ND indicates not detected.

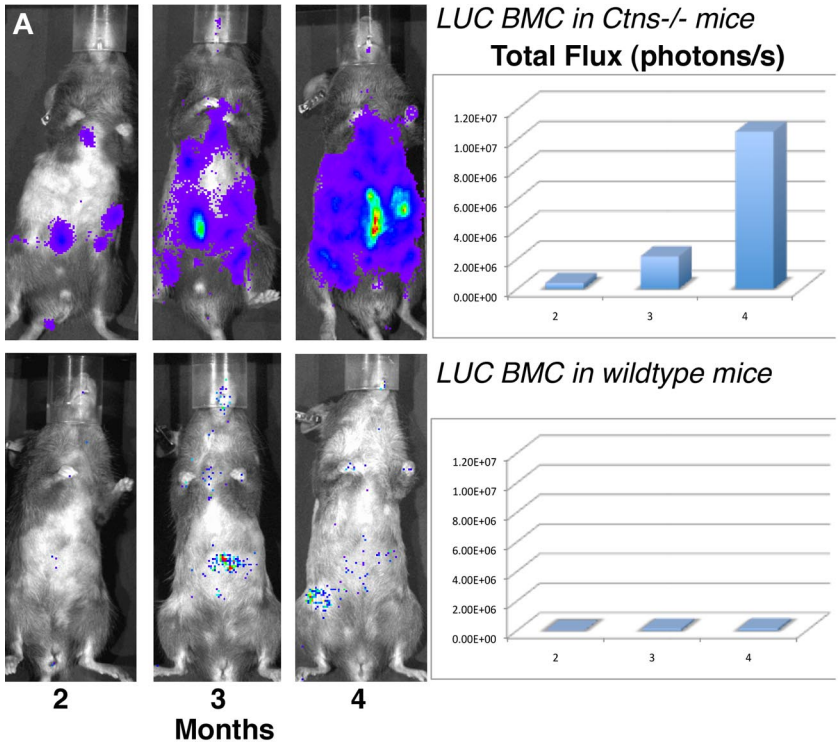

B

	Percent of *Ctns* expression*	
	2 months	4 months
Brain	1.7	5.9
Eye	10.6	13.4
Heart	8.0	11.0
Kidney	2.1	12.9
Liver	1.7	9.6
Muscle	0.9	5.4
Spleen	0.7	19.3

*Percent of *Ctns* expression in $Ctns^{-/-}$ mice treated with WT BMC compared to wildtype mice.

Figure 6. In vivo luciferase imaging and quantitative *Ctns* expression in $Ctns^{-/-}$ mice treated with WT BMCs as a function of time. (A) BMCs isolated from luciferase transgenic mice were transplanted into lethally irradiated $Ctns^{-/-}$ mice (top panel) and WT mice (bottom panel). These are representative pictures taken in live animals with the IVIS imaging system after luciferin injection at 2, 3, and 4 months. The luminescence signal intensities were quantified and are represented in the matching histograms. (B) Percentage of *Ctns* expression in $Ctns^{-/-}$ mice treated with WT BMCs compared with WT mice. The results represent the number of *Ctns* gene copies determined by quantitative RT-PCR as a ratio of the results shown in Table 3 for BMC-treated $Ctns^{-/-}$ mice divided by the results for WT control mice.

tubular cells.[25,26] $Ctns^{-/-}$ mice develop an incomplete renal disease, but like the human patients, cystine crystals accumulate progressively within interstitial cells.[14] Thus, BMC-derived interstitial cells in our transplanted mice may have a significant, positive effect on the progression of the underlying kidney disease.

On the other hand, MSCs did not integrate efficiently within the kidney in our model. Nonetheless, MSC transplantation led to some improvement in renal function compared with control $Ctns^{-/-}$ mice transplanted with $Ctns^{-/-}$ BMCs. However, after an initial decrease in cystine content at 2 months, cystine levels increased thereafter. In the literature, the potential for MSC transplantation to improve kidney failure remains controversial. Several studies showed that, in the setting of renal injury, transplanted MSCs can generate mesangial and tubular epithelial cells[27] and restore renal structure and function.[28,29] Others showed that MSC injections do not prevent Alport syndrome in COL4A3-deficient mice and MSCs do not differentiate into renal cells.[30] The protective effects of MSCs seem to be the result of a paracrine effect of these cells by secretion of growth factors, such as vascular endothelial growth factor and transforming growth factor-β1, rather than cellular differentiation.[31,32] This mechanism could explain the initial improvement we observed in the $Ctns^{-/-}$ mice.

We evaluated the engraftment of BMC-derived cells in multiple tissues based on 3 metrics: GFP-positive cells identified by confocal microscopy, quantitative PCR for *Ctns* expression, and cystine content determined by mass spectrometry. The results by all these metrics showed high levels of engraftment in eye, brain, muscle, liver, spleen, and heart. The nature of cystinosis as a clinical entity is a progressive dysfunction of multiple organs caused by the accumulation of cystine in the tissues; thus, the findings here underline the potential utility of BMC transplantation for this genetic disease. Of particular importance is that, although cystine levels continued to increase in the $Ctns^{-/-}$ mice as a function of time, our data demonstrated that successful transplantation of WT BMCs reversed this accumulation.

Table 4. *Ctns* expression in the different tissues of mice treated with $Sca1^+$ HSC compared with wild-type and $Ctns^{-/-}$ controls

Relative expression of *Ctns* as fold changes*	Wild-type mice	$Ctns^{-/-}$ mice	$Ctns^{-/-}$ mice $Sca1^+$ HSC	Percentage *Ctns* in Sca1-transplanted vs wild-type mice
Brain	93 381 ± 93 056	ND	1940 ± 2201	2.1
Eye	780 359 ± 899 835	ND	34 532 ± 26 910	4.4
Heart	204 857 ± 143 183	ND	8725 ± 3488	4.3
Kidney	72 120 ± 36 321	ND	6291 ± 7818	8.7
Liver	26 656 ± 21 901	ND	3588 ± 2558	13.5
Muscle	46 125 ± 11 840	ND	3288 ± 2923	7.1
Spleen	19 634 ± 3603	ND	15 218 ± 3590	77.5

ND indicates not detected.
*18S-normalized fold changes.

Table 5. Cystine content in the different tissues of mice treated with Sca1$^+$ HSC compared with wild-type and Ctns$^{-/-}$ controls

Cystine content, nmol half-cystine/mg protein	Wild-type mice	Ctns$^{-/-}$ mice	Ctns$^{-/-}$ mice Sca1$^+$ HSC	Percentage cystine decrease in Sca1-transplanted vs Ctns$^{-/-}$ mice
Brain	0.02 ± 0.01	1.33 ± 0.40	0.57 ± 0.13*	57.5
Eye	0.04 ± 0.01	47.46 ± 14.95	9.25 ± 1.33*	80.5
Heart	0.14 ± 0.05	58.85 ± 14.28	5.48 ± 2.33*	90.7
Kidney	0.19 ± 0.06	112.85 ± 59.72	63.72 ± 49.40*	43.5
Liver	0.02 ± 0.01	60.21 ± 20.58	4.07 ± 1.83*	93.2
Muscle	0.22 ± 0.10	29.19 ± 9.96	6.71 ± 1.44*	77.0
Spleen	0.06 ± 0.03	168.75 ± 52.08	16.76 ± 16.69*	90.1

*$P < .05$ vs Ctns$^{-/-}$ control mice.

In patients, corneal cystine crystals appear from the first decade of life, resulting in photophobia and visual impairment.[4] Cystine crystals are found first in the periphery of the cornea and then in the center.[33] *Ctns*$^{-/-}$ mice demonstrate similar ocular anomalies to patients,[14,34] and cystine crystals are also first found at the periphery of the cornea. In addition to the decreased cystine content, BMC transplantation led to a significant decrease in the number of mice with corneal cystine crystals (43% WT BMCs vs 86% of Ctns$^{-/-}$ BMCs; $P < .05$). In the third decade of life, patients with cystinosis exhibit a deterioration of the central nervous system characterized by mental deterioration, impaired cerebellar function, pyramidal signs, ischemic lesions, and severe impairment in visual short-term memory.[4] Middle-aged *Ctns*$^{-/-}$ mice also present with behavioral anomalies and spatial and working memory deficits that correlate with cystine accumulation in the brain.[14,35] In the present study, we demonstrated *Ctns* expressing BMC-derived cells in the brain, differentiated into or fused with endothelial or smooth muscle cells, as well as some glial-like cells. For another LSD, metachromatic leukodsytrophy, partial[36] or total[37] correction was observed after BMC transplantation in the mouse model. BMC-derived cells repopulated the central nervous system microglia.[37] For α-mannosidosis, functional enzyme was present in neurons, glial cells, and cells associated with blood vessels after BMC transplantation in kittens lacking α-mannosidosase.[38]

Without cysteamine, cystinotic patients develop myopathy with atrophy and progressive distal extremity weakness as well as progressive oromotor dysfunction, including dysphagia.[4] Cystine crystals were observed in fibroblastic cells adjacent to muscle fibers and within perimysial collagen fibrils, and muscle necrosis was also observed.[39] The *Ctns*$^{-/-}$ mice also present with muscular impairment associated with cystine crystals located in interstitial cells and myocyte necrosis.[14] Cardiomyopathy can be a late complication in cystinosis,[4] and one autopsy revealed the presence of cystine crystals in interstitial cardiac histiocytes and one myocardial cell.[40] Similarly, crystals were abundant in interstitial cells of *Ctns*$^{-/-}$ mice heart but not in myocytes.[14] In our data, *Ctns*-expressing BMC-derived cells in heart and skeletal muscle were mostly interstitial, although some GFP-positive muscle fibers were present. The spleen was the organ in which we found the most abundant amount of *Ctns*-expressing BMC-derived cells. Curiously, most of these cells were not of lymphoid lineage but rather part of the reticuloendothelial system. Some patients require a splenectomy because of accumulation of cystine crystals in endothelial cells and macrophages in the spleen.[41] Finally, cystine crystals are found in Kupffer cells in the liver of patients.[41] Our results show that *Ctns*-expressing BMC-derived cells in the liver were essentially all Kupffer cells.

Only engraftment of bone marrow cells producing a functional *Ctns* was able to reverse the disease process and reduce tissue cystine levels in our model as *Ctns*$^{-/-}$ mice transplanted with Ctns$^{-/-}$ BMCs still accumulated cystine and developed kidney dysfunction. The fact that lethally irradiated WT mice exhibited few transplanted BMC-derived cells in the tissues, as shown by confocal microscopy for GFP-positive cells and IVIS imaging for luciferase-expressing cells, proves that the extensive colonization of *Ctns*$^{-/-}$ mice by WT BMC-derived cells is specifically the result of the impact of cystinosis. The few BMC-derived cells observed in WT mice might be myeloid and lymphoid lineage fusion hybrids that can occur after lethal irradiation of mice.[42] In contrast, *Ctns*$^{-/-}$ mice exhibited abundant BMC-derived cells (eg, GFP-positive) that colocalized with tissue-specific cell phenotypes, and the studies of luciferase BMC-derived cells in live animals confirmed the increase in engraftment over time. Moreover, most of these cells were not from the lymphoid lineage (specifically, not macrophages), even in the spleen, but were part of the intrinsic structure of the organ. Tissue engraftment of bone marrow–derived cells can occur through cell differentiation or cell fusion.[43] For instance, bone marrow cells can give rise to endothelial, smooth muscle reticuloendothelial, and Kupffer cells through differentiation[44-46] and skeletal muscle through fusion.[47] However, this field is still controversial[48,49]; and, in our case, the mechanism remains to be established.

Taken together, the literature on cystinosis and our data indicate that *Ctns* expressing BMC replace or fuse with cells that accumulate the most cystine crystals in each tissue. Thus, BMC transplantation creates a reservoir of healthy cells that migrate to the targeted organ as a function of progressive cellular injury and may replace or fuse with the cells accumulating the highest levels of cystine, many of which are interstitial and reticuloendothelial cells. Consistent with this conclusion, Hippert et al depleted 75% of the liver cystine content in *Ctns*$^{-/-}$ mice by chemically depleting Kupffer cells representing less than 10% of the total cells in the liver.[15] It is also interesting to note that the addition of the *CTNS* gene to *Ctns*$^{-/-}$ hepatocytes in culture resulted in a significant decrease in cystine levels.[15] We have confirmed these experiments using *Ctns*$^{-/-}$ fibroblasts (data not shown). In sum, these data add additional support to the conclusion that there is a direct relationship between expression of a functional protein and the reduction in cystine levels.

Cystinosin is a transmembrane protein localized to the intracellular lysosomal membrane. Thus, cells lacking *Ctns* cannot recapture the normal protein from transplanted WT cells, even in close proximity. In contrast, in Hurler syndrome, normal enzyme can be secreted by BMC tissue-engrafted cells and taken up by adjacent host cells. Indeed, in a murine model of Hurler syndrome treated by transplantation of retroviral-transduced bone marrow cells, tissue engraftment of transgene-positive cells was low, primarily limited to spleen and liver. Nonetheless, glycosaminoglycan levels decreased in all the tissues tested, and that effect was explained by

uptake of the secreted enzyme by adjacent cells.[50,51] In contrast, in our studies, the mechanism underlying the decrease of cystine in all tissues involves the localization of cells expressing the functional gene and, thus, is correlated with the abundant engraftment of BMC-derived cells. Therefore, BMC transplantation for cystinosis is an example where therapeutic efficacy requires the local integration of cells with the functional protein rather than local delivery of a missing enzyme like many LSDs.

HSC transplantation, modeled in mice by purification of $Sca1^+$ HSCs, has the same therapeutic effects as whole bone marrow cell transplantation in the mouse model of cystinosis, including high levels of tissue engraftment and significant decreases in cystine content. This is important because human HSCs ($CD34^+$) are readily isolated from peripheral blood after growth factor-mediated mobilization (ie, granulocyte-macrophage colony-stimulating factor) and this population is significantly enriched for the true HSCs. Moreover, future ex vivo gene delivery to introduce a functional *Ctns* gene will be more efficient with purified HSCs than with whole BMCs.

This work represents the first step toward a clinical trial of using bone marrow cell transplantation as a therapy for cystinosis. This disease, like many lysosomal storage disorders, is a slowly progressive process that represents an ongoing cystine accumulation, leading downstream to cell stress, cell death, tissue injury, and eventually organ dysfunction, including kidney failure, blindness, and progressive myopathy. The permanent engraftment of bone marrow cells expressing a fully functional *CTNS* gene would provide a continuous source of healthy cells that could traffic to different tissue compartments where cells are stressed or dying from cystine accumulation. We have demonstrated the high efficiency of this strategy in the cystinosis model as determined objectively by significant levels of bone marrow–derived cell engraftment in multiple tissue compartments correlated with improvements in measured cystine content and renal function. These results suggest that bone marrow cell or hematopoietic stem cell transplantation is particularly suitable for the chronic and progressive injury characteristic of cystinosis and potentially other lysosomal storage disorders in which mutations of intracellular and transmembrane proteins are involved.

Acknowledgments

The authors thank Dr Corinne Antignac for providing the Ctns $^{-/-}$ mice, Dr Michael Geusz for the luciferase transgenic mice, and Dr Marie-Claire Gubler for expert assistance with the kidney histology.

This work was supported by the Cystinosis Research Foundation and the Molly Baber Research Fund.

Authorship

Contribution: K.S., F.H., M.T., and S.C. performed research and analyzed data; S.C. and D.R.S. designed the project and wrote the manuscript; J.V.J. and J.S. performed the eye analysis; and S.R. contributed to the brain analysis.

Conflict-of-interest disclosure: The authors declare no competing financial interests.

Correspondence: Stephanie Cherqui, Department of Molecular and Experimental Medicine, Scripps Research Institute, 10550 North Torrey Pines Rd, La Jolla, CA 92037; e-mail: scherqui@scripps.edu.

References

1. Town M, Jean G, Cherqui S, et al. A novel gene encoding an integral membrane protein is mutated in nephropathic cystinosis. *Nat Genet.* 1998;18:319-324.
2. Cherqui S, Kalatzis V, Trugnan G, Antignac C. The targeting of cystinosin to the lysosomal membrane requires a tyrosine-based signal and a novel sorting motif. *J Biol Chem.* 2001;276:13314-13321.
3. Kalatzis V, Cherqui S, Antignac C, Gasnier B. Cystinosin, the protein defective in cystinosis, is a H(+)-driven lysosomal cystine transporter. *EMBO J.* 2001;20:5940-5949.
4. Nesterova G, Gahl W. Nephropathic cystinosis: late complications of a multisystemic disease. *Pediatr Nephrol.* 2008;23:863-878.
5. North American Pediatric Renal Trials and Collaborative Studies. NAPRTCS 2008 Annual Report. https://web.emmes.com/study/ped/annlrept/annlrept.html. Accessed May 2009.
6. Gahl WA, Thoene JG, Schneider JA. Cystinosis. *N Engl J Med.* 2002;347:111-121.
7. Pastores GM, Barnett NL. Current and emerging therapies for the lysosomal storage disorders. *Expert Opin Emerg Drugs.* 2005;10:891-902.
8. Kleta R, Gahl WA. Pharmacological treatment of nephropathic cystinosis with cysteamine. *Expert Opin Pharmacother.* 2004;5:2255-2262.
9. Krivit W. Allogeneic stem cell transplantation for the treatment of lysosomal and peroxisomal metabolic diseases. *Springer Semin Immunopathol.* 2004;26:119-132.
10. Peters C, Steward CG. Hematopoietic cell transplantation for inherited metabolic diseases: an overview of outcomes and practice guidelines. *Bone Marrow Transplant.* 2003;31:229-239.
11. Braunlin EA, Rose AG, Hopwood JJ, Candel RD, Krivit W. Coronary artery patency following long-term successful engraftment 14 years after bone marrow transplantation in the Hurler syndrome. *Am J Cardiol.* 2001;88:1075-1077.
12. Peters C, Shapiro EG, Anderson J, et al. Hurler syndrome: II. Outcome of HLA-genotypically identical sibling and HLA-haploidentical related donor bone marrow transplantation in fifty-four children: the Storage Disease Collaborative Study Group. *Blood.* 1998;91:2601-2608.
13. Staba SL, Escolar ML, Poe M, et al. Cord-blood transplants from unrelated donors in patients with Hurler's syndrome. *N Engl J Med.* 2004;350:1960-1969.
14. Cherqui S, Sevin C, Hamard G, et al. Intralysosomal cystine accumulation in mice lacking cystinosin, the protein defective in cystinosis. *Mol Cell Biol.* 2002;22:7622-7632.
15. Hippert C, Dubois G, Morin C, et al. Gene transfer may be preventive but not curative for a lysosomal transport disorder. *Mol Ther.* 2008;16:1372-1381.
16. Meirelles Lda S, Nardi NB. Murine marrow-derived mesenchymal stem cell: isolation, in vitro expansion, and characterization. *Br J Haematol.* 2003;123:702-711.
17. Schneider JA. Approval of cysteamine for patients with cystinosis. *Pediatr Nephrol.* 1995;9:254.
18. Cantley LG. Adult stem cells in the repair of the injured renal tubule. *Nat Clin Pract Nephrol.* 2005;1:22-32.
19. Kale S, Karihaloo A, Clark PR, Kashgarian M, Krause DS, Cantley LG. Bone marrow stem cells contribute to repair of the ischemically injured renal tubule. *J Clin Invest.* 2003;112:42-49.
20. Poulsom R, Forbes SJ, Hodivala-Dilke K, et al. Bone marrow contributes to renal parenchymal turnover and regeneration. *J Pathol.* 2001;195:229-235.
21. Ito T, Suzuki A, Imai E, Okabe M, Hori M. Bone marrow is a reservoir of repopulating mesangial cells during glomerular remodeling. *J Am Soc Nephrol.* 2001;12:2625-2635.
22. Sugimoto H, Mundel TM, Sund M, Xie L, Cosgrove D, Kalluri R. Bone-marrow-derived stem cells repair basement membrane collagen defects and reverse genetic kidney disease. *Proc Natl Acad Sci U S A.* 2006;103:7321-7326.
23. Lin F, Moran A, Igarashi P. Intrarenal cells, not bone marrow-derived cells, are the major source for regeneration in postischemic kidney. *J Clin Invest.* 2005;115:1756-1764.
24. Duffield JS, Park KM, Hsiao LL, et al. Restoration of tubular epithelial cells during repair of the postischemic kidney occurs independently of bone marrow-derived stem cells. *J Clin Invest.* 2005;115:1743-1755.
25. Mahoney CP, Striker GE. Early development of the renal lesions in infantile cystinosis. *Pediatr Nephrol.* 2000;15:50-56.
26. Spear GS, Gubler MC, Habib R, Broyer M. Renal allografts in cystinosis and mesangial demography. *Clin Nephrol.* 1989;32:256-261.
27. Yokoo T, Sakurai T, Ohashi T, Kawamura T. Stem cell gene therapy for chronic renal failure. *Curr Gene Ther.* 2003;3:387-394.
28. Herrera MB, Bussolati B, Bruno S, Fonsato V, Romanazzi GM, Camussi G. Mesenchymal stem cells contribute to the renal repair of acute tubular epithelial injury. *Int J Mol Med.* 2004;14:1035-1041.
29. Morigi M, Imberti B, Zoja C, et al. Mesenchymal stem cells are renotropic, helping to repair the

kidney and improve function in acute renal failure. *J Am Soc Nephrol.* 2004;15:1794-1804.

30. Ninichuk V, Gross O, Segerer S, et al. Multipotent mesenchymal stem cells reduce interstitial fibrosis but do not delay progression of chronic kidney disease in collagen4A3-deficient mice. *Kidney Int.* 2006;70:121-129.
31. Kunter U, Rong S, Djuric Z, et al. Transplanted mesenchymal stem cells accelerate glomerular healing in experimental glomerulonephritis. *J Am Soc Nephrol.* 2006;17:2202-2212.
32. Togel F, Cohen A, Zhang P, Yang Y, Hu Z, Westenfelder C. Autologous and allogeneic marrow stromal cells are safe and effective for the treatment of acute kidney injury. *Stem Cells Dev.* 2008;18:475-485.
33. Melles RB, Schneider JA, Rao NA, Katz B. Spatial and temporal sequence of corneal crystal deposition in nephropathic cystinosis. *Am J Ophthalmol.* 1987;104:598-604.
34. Kalatzis V, Serratrice N, Hippert C, et al. The ocular anomalies in a cystinosis animal model mimic disease pathogenesis. *Pediatr Res.* 2007;62:156-162.
35. Maurice T, Hippert C, Serratrice N, et al. Cystine accumulation in the CNS results in severe age-related memory deficits. *Neurobiol Aging.* 2009; 30:987-1000.
36. Matzner U, Hartmann D, Lullmann-Rauch R, et al. Bone marrow stem cell-based gene transfer in a mouse model for metachromatic leukodystrophy: effects on visceral and nervous system disease manifestations. *Gene Ther.* 2002;9:53-63.
37. Biffi A, De Palma M, Quattrini A, et al. Correction of metachromatic leukodystrophy in the mouse model by transplantation of genetically modified hematopoietic stem cells. *J Clin Invest.* 2004;113: 1118-1129.
38. Walkley SU, Thrall MA, Dobrenis K, et al. Bone marrow transplantation corrects the enzyme defect in neurons of the central nervous system in a lysosomal storage disease. *Proc Natl Acad Sci U S A.* 1994;91:2970-2974.
39. Charnas LR, Luciano CA, Dalakas M, et al. Distal vacuolar myopathy in nephropathic cystinosis. *Ann Neurol.* 1994;35:181-188.
40. Dixit MP, Greifer I. Nephropathic cystinosis associated with cardiomyopathy: a 27-year clinical follow-up. *BMC Nephrol.* 2002;3:8.
41. Gagnadoux MF, Tete MJ, Guest G, Arsan A, Broyer M. Hepatosplenic disorders in nephropatic cystinosis. In: Broyer M, ed. *Cystinosis.* Amsterdam, The Netherlands: Elsevier; 1999:70-74.
42. Nygren JM, Liuba K, Breitbach M, et al. Myeloid and lymphoid contribution to non-haematopoietic lineages through irradiation-induced heterotypic cell fusion. *Nat Cell Biol.* 2008;10:584-592.
43. Pessina A, Gribaldo L. The key role of adult stem cells: therapeutic perspectives. *Curr Med Res Opin.* 2006;22:2287-2300.
44. Bailey AS, Willenbring H, Jiang S, et al. Myeloid lineage progenitors give rise to vascular endothelium. *Proc Natl Acad Sci U S A.* 2006;103:13156-13161.
45. Tanaka K, Sata M. Contribution of circulating vascular progenitors in lesion formation and vascular healing: lessons from animal models. *Curr Opin Lipidol.* 2008;19:498-504.
46. Klein I, Cornejo JC, Polakos NK, et al. Kupffer cell heterogeneity: functional properties of bone marrow derived and sessile hepatic macrophages. *Blood.* 2007;110:4077-4085.
47. Sherwood RI, Christensen JL, Weissman IL, Wagers AJ. Determinants of skeletal muscle contributions from circulating cells, bone marrow cells, and hematopoietic stem cells. *Stem Cells.* 2004;22:1292-1304.
48. Kashofer K, Bonnet D. Gene therapy progress and prospects: stem cell plasticity. *Gene Ther.* 2005;12:1229-1234.
49. Quesenberry PJ, Dooner G, Colvin G, Abedi M. Stem cell biology and the plasticity polemic. *Exp Hematol.* 2005;33:389-394.
50. Di Domenico C, Villani GR, Di Napoli D, et al. Gene therapy for a mucopolysaccharidosis type I murine model with lentiviral-IDUA vector. *Hum Gene Ther.* 2005;16:81-90.
51. Zheng Y, Rozengurt N, Ryazantsev S, Kohn DB, Satake N, Neufeld EF. Treatment of the mouse model of mucopolysaccharidosis I with retrovirally transduced bone marrow. *Mol Genet Metab.* 2003;79:233-244.